PIER M

Stack Dual-Band EBG Based Sensor for Dielectric Characterization of Liquids

Pramod P. Bhavarthe[1, *], Alam N. Shaikh[2], and Kompella S. L. Parvathi[2]

[1]*Department of Electronics & Telecommunication Engineering, Shah & Anchor Kutchhi Engineering College*
University of Mumbai, Mumbai, Maharashtra, India
[2]*Department of Artificial Intelligence and Data Science, Vasantdada Patil Pratishthan's College of Engineering and Visual Arts*
University of Mumbai, Mumbai, Maharashtra, India

ABSTRACT: A tiny electromagnetic band gap (EBG) based microwave sensor with dual-band operation for dielectric characterization of Liquids is presented in this work. The suggested design uses a suspended microstrip line placed over the stack dual-band type EBG (SD-EBG) unit cell at 2.40 GHz and 2.98 GHz. To achieve the dual band characteristics, the stack type of EBG with different patch sizes and offset vias is used. To validate the sensor performance, absolute solution of butan-l-o1, methonal, and water are considered as liquid under test (LUT) and loaded in transparent polypropylene (PP) material, and the maximum sensitivity of 1.14% from the first resonance with maximum Q-factor of 137.5 from the second resonance is achieved with frequency detection resolution of 27.4 MHz. The size of proposed SD-EBG based sensor is 54.95% and 39.02% of that of planar EBG based sensor and cesaro fractals EBG based sensor.

1. INTRODUCTION

Complex permittivity is a key and important property of liquid which defines the electromagnetic response. Dielectric properties of liquid are important in many industries, including food [1, 2] and medicine [3, 4]. They help to determine quality and characteristics of these liquids. By measuring dielectric properties, we can asses factors like electrical conductivity, permittivity, and loss tangent [5, 6]. These measurements provide valuable insights for ensuring the safety and effectiveness of products in various applications. These metrics offer valuable insights regarding product safety and effectiveness in numerous applications. In recent years, optical and sensor-based technologies for liquid characterization have advanced. These technologies are popular because they are sensitive and efficient at detecting and analyzing liquid characteristics. It is important to recognize that these methods might be complicated, expensive, and limit liquid reuse after testing [7]. Microwave sensors have become popular due to their simplicity and ability to overcome other sensing obstacles. Their capacity to penetrate various substrates, including liquids, makes them useful in industrial process, food monitoring, and medical diagnosis [7]. The literature showcases that the utilization of both non-resonance [8, 9] and resonance based [10–20] microwave sensors tends to be favoured due to their heightened precision and accuracy. Notably, the implementation of split-ring resonator (SRR) [12–14], complementary split-ring resonator (CSRR) [15, 16] as sensing element, and multi-band sensors [19, 21, 22] has been extensively documented for the purpose of calculating and evaluating the characteristics of liquids. Single-band gap electromagnetic band gap (EBG) based

sensors [7, 23–26] are proposed for characterizing various liquids under test (LUT). Central located via EBG (CLV-EBG) based sensor [25] is introduced for measuring permittivity of industrial liquids. Parallel tapper lines are employed in resonance detection with overall size of $70 \text{ mm} \times 140 \text{ mm}$. Theis sensor configuration comprises 2×7 EBG arrays resulting in an increased overall size. This design is particularly effective for measuring low range permittivity of the LUT. In [26], an approach was proposed for liquid detection using a multilayer planner EBG based sensor. The EBG surface was ingeniously modified by incorporating trenches between square EBG cells, effectively transforming it into sensor. These trenches were then selectively filled with different LUT, each possessing distinct dielectric properties. The EBG surface is strategically positioned beneath a coplanar waveguide (CPW) antenna to serve as a radiating source. This configuration enables the detection of resonance changes within the EBG cells when different LUT materials are introduced. However, it is important to note that the use of 3×3 EBG cells results in an increased overall size. This approach may have limitations such as reduced detection range of dielectric constant (ϵ_r) and a lower quality factor. In [7], a Cesaro fractal EBG sensor is proposed for LUT material characterization. The sensor consists of a 3×3 array of Cesaro fractal EBG planes, along with a triangle-shaped patch antenna. However, it should be noted that the use of a 3×3 array of EBG planes increases the overall size of the sensor. Consequently, the development of such a multi-band sensor with a minimal resonator configuration holds great promise for advancing the field of material characterization.

This work proposes a dual band stack EBG microwave sensor with compact size, high-sensitivity, and wide-range measurement of ϵ_r in LUT dielectric characterization. The paper's

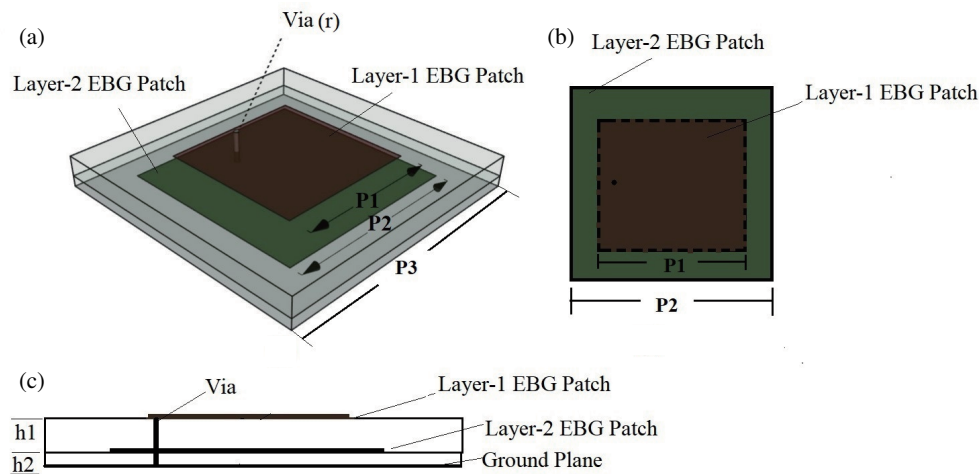* Corresponding author: Pramod P. Bhavarthe (ppbhavarthe@gmail.com).

FIGURE 1. Geometry of SD-EBG. (a) 3-D geometry, (b) Top view, and (c) Side view. $(P_1, P_2, P_3\ h_1, h_2, r, \epsilon_r) = (10.0\,\text{mm}, 14.5\,\text{mm}, 19.5\,\text{mm}, 1.575\,\text{mm}, 0.787\,\text{mm}, 0.2\,\text{mm}, 2.2,)$.
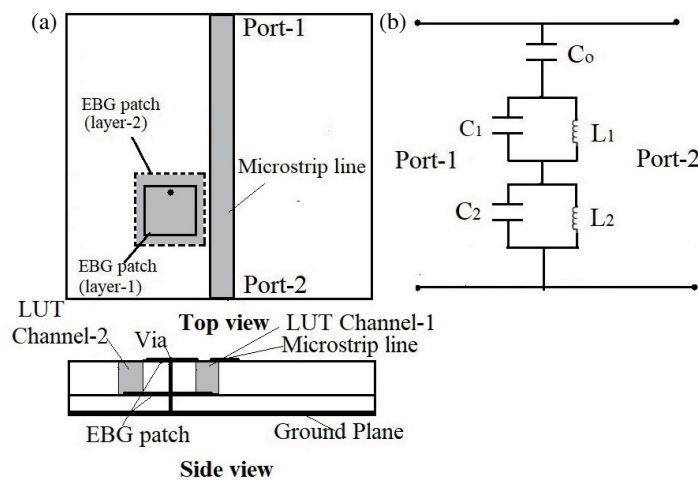

FIGURE 2. Microstrip-line-based model of SD-EBG structure. (a) Configuration schematic view, and (b) Equivalent-circuit.

structure is as follows. Section 2 covers SD-EBG unit cell characteristics and shape. Design and functioning of the dual-band sensor are described in Section 3, including experimental measurements. The proposed EBG-based sensor is analyzed in Section 4 and reported in Section 5.

2. DESIGN OF EBG CELL AND DISPERSION DIAGRAM

Figure 1 shows the geometry of the unit cell of the stack dual band type EBG (SD-EBG). The dual band gap is achieved by using lower and upper EBG patches with distinct periodic sizes. It is designed on a substrate with dielectric constant $(\epsilon_r) = 2.2$ and loss tangent $(\tan \delta) = 0.0009$. Layer-1 and layer-2 are with height $(h_1) = 1.575$ mm and $(h_2) = 0.787$ mm, respectively. The other parameters of the SD-EBG are mentioned in Fig. 1. Microstrip line based equivalent circuit model [27] of the SD-EBG is shown in Fig. 2 as this approach is applied when only one cell of EBG is adequate in application [27]. As shown in Figs. 2(a) and (b), the capacitance C_o is due to fringing effect between upper EBG patch and microstrip line present at the same plane.

Upper EBG patch and Lower EBG patch give the capacitance C_1, and similarly, capacitance C_2 is due to lower EBG patch and ground plane. From equivalent circuit, it is clear that two parallel LC circuits per unit cell [28] give dual band characteristics of SD-EBG. Periodic size of the lower EBG compared to the upper EBG patch is more; therefore, the first resonance is due to lower EBG patch. The surface impedance (Z) of the EBG is given as [29, 30]

$$Z = \frac{j\omega L}{1 - \omega^2 LC} \tag{1}$$

and

$$BW = \frac{1}{\eta_0}\sqrt{\frac{L}{C}} \tag{2}$$

where the resonance frequencies (f_{01}) and (f_{02}) of each band are given as [29, 30]

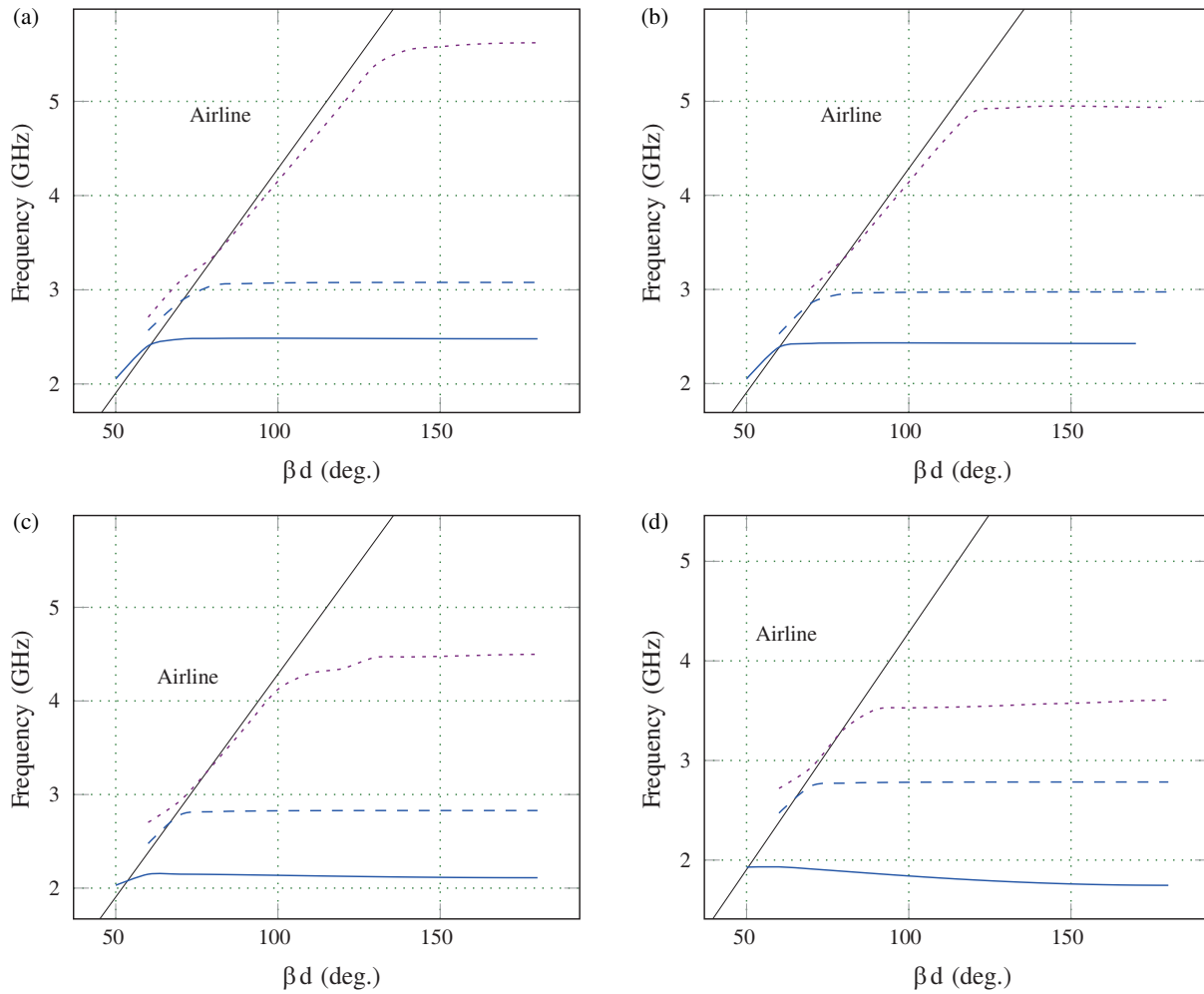$$f_{o1} = \frac{1}{2\pi\sqrt{L_1 C_1}} \tag{3}$$

FIGURE 3. Dispersion diagrams of SD-EBG for different LUT loaded in channel. (a) No sample ($\epsilon_r = 1$), (b) Butan-1-ol ($\epsilon_r = 3.55$), (c) Methanol ($\epsilon_r = 22.38$), and (d) water ($\epsilon_r = 78.8$). (——— mode 1, – – – mode 2, $\cdots\cdots$ mode 3).

$$f_{o2} = \frac{1}{2\pi\sqrt{L_2 C_2}} \qquad (4)$$

where η_0 is the free space impedance. From (3) and (4), to vary f_{01} and f_{02}, values of C_1 and C_2 should be varied. To vary C_1 and C_2, trenches are created near the EBG patch as shown in Fig. 1 and Fig. 2. The change in the effective ϵ_r results in the variation of C_1 and C_2. To study the variation in f_{01} and f_{02} due to the change in C_1 and C_2, unit cell of the SD-EBG is simulated in eigen-mode solution of Ansys high frequency structure simulator (HFSS) [31]. The different parameters of the unit cell of SD-EBG are mentioned in Fig. 1. The trenches are filled with materials of dielectric constant $\epsilon_r = 1$, 3.55, 22.38, 78.8 [32, 33], and dispersion diagrams are shown in the Figs. 3(a), (b), (c), and (d), respectively. As shown in Fig. 3, band gap center frequency for the first band changes from 2.54 GHz to 2.15 GHz and for second band from 2.97 GHz to 2.54 GHz for ϵ_r range from 1 to 78.8. To study the effect of trenches height, the simulations are also done for different h_2, and very small variation in both resonance frequencies with less effect on the bandwidth is observed. To study the effect of change in the loss tangent, trenches are filled with different materials with loss tangent from 0 to 0.9 with $\epsilon_r = 2$, and it is observed that the change in loss tangent has no noticeable effect on both resonance frequency bands of the SD-EBG.

3. PROPOSED SENSOR DESIGN AND EXPERIMENTAL RESULTS

3.1. Sensor Design and Simulated Results

The proposed EBG based sensor is shown in Fig. 4 with unit cell of SD-EBG. The substrate with specification $\epsilon_r = 2.2$, $\tan\delta = 0.0009$, $h_1 = 0.787\,\text{mm}$, $h_2 = 1.575\,\text{mm}$ is used in simulation. The overall size of the sensor is $50\,\text{mm} \times 40\,\text{mm}$ with lower EBG patch and upper EBG patch size $15\,\text{mm} \times 15\,\text{mm}$ and $10.5\,\text{mm} \times 10.5\,\text{mm}$, respectively. Other dimension of the SD-EBG are kept the same as mentioned in previous section. The stopband characteristics of SD-EBG structure are used to measure the dielectric properties of the LUT [7, 26]. In the proposed sensor, a suspended microstrip line [34] is used as a sensing element to sense the resonance of SD-EBG for different LUT. A $50\,\Omega$ microstrip
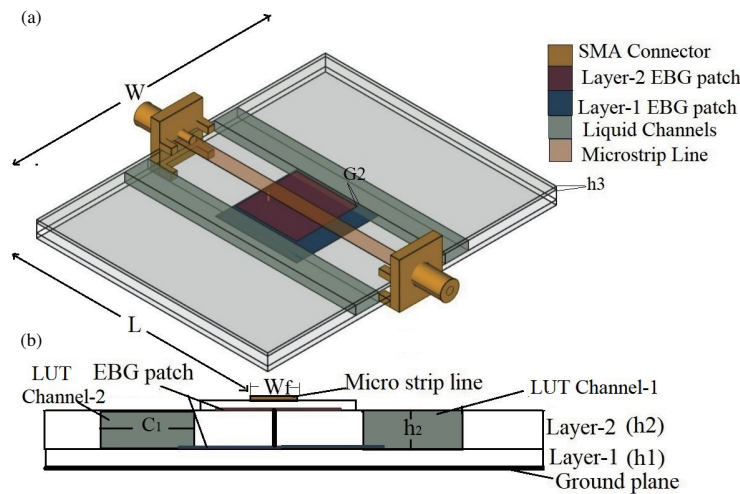
FIGURE 4. Geometry of proposed SD-EBG based microwave sensor $(W, L, G_2, \epsilon_r, h_1, h_2, h_3, C_2, W_f, P_1, P_2, r)$ = (50.0 mm, 40.0 mm, 0.5 mm, 2.2, 0.787 mm, 1.575 mm, 0.5 mm, 4 mm, 2.46 mm, 10.00 mm, 14.5 mm, 0.2 mm).
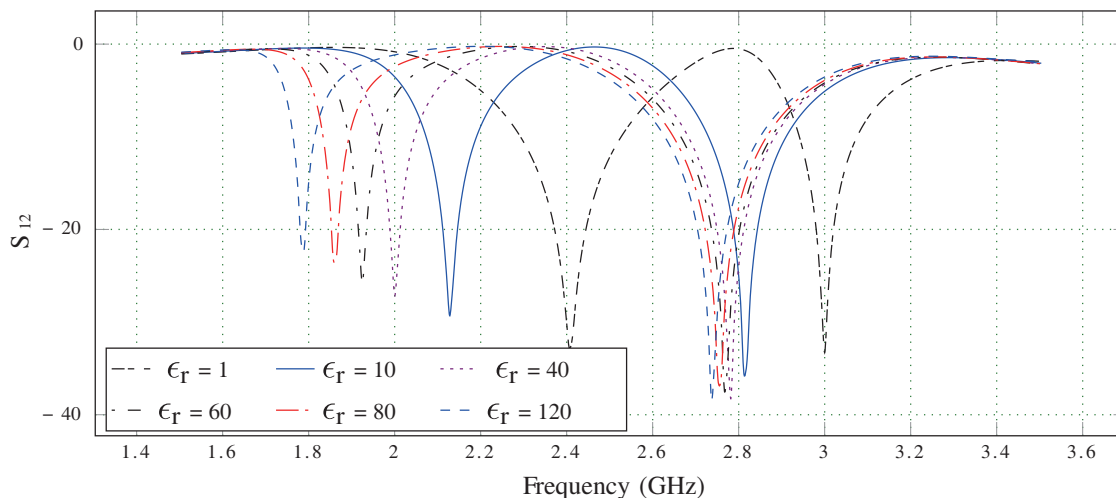

FIGURE 5. Simulated dependence of S_{12} of proposed sensor on dielectric constant (ϵ_r) with $\tan\delta = 0$.

line is placed above the SD-EBG as shown in Fig. 4. To place the LUT, trenches as shown in the Fig. 4 of size $4\,\text{mm} \times 1.5\,\text{mm}$ are created with gap 1 mm from upper EBG patch. In comparison point view, the sizes of trenches are kept the same as mentioned in [7]. The proposed sensor is simulated using Ansys HFSS. To access the frequency tuning capability of the proposed sensor, the structure is simulated when the trenches are filled with different ϵ_r and $\tan\delta$ values. The ϵ_r from 1 to 120 with $\tan\delta = 0$ [26] is kept fixed, and simulated S_{12} is shown in Fig. 5. f_{01} and f_{02} are tuned down when ϵ_r increases as shown in Fig. 6(a). For $\epsilon_r = 1$, 10, 40, 60, 80, and 120, f_{01} and f_{02} are observed at 2.45 GHz, 2.12 GHz, 2.00 GHz, 1.92 GHz, 1.86 GHz, 1.78 GHz and 2.99 GHz, 2.81 GHz, 2.78 GHz, 2.76 GHz, 2.75 GHz, 2.73 GHz, respectively. In order to study the effect of $\tan\delta$, the $\tan\delta$ of each trench is varied from 0 to 0.9 with $\epsilon_r = 2$ [26], and simulated results are shown in Fig. 6(b). As shown in Fig. 6(b), f_{01} and f_{02} are almost the same with noticeable changes in $-3\,\text{dB}$ bandwidth observed for different $\tan\delta$ values.

3.2. Experimental Results

Figures 7 and 8 show the prototype of fabricated sensor and experiment setup. The proposed sensor is printed on a Rogers RT/duroid 5880 (tm) substrate with $\epsilon_r = 2.2$, $\tan\delta = 0.0009$, $h_1 = 1.575\,\text{mm}$, and $h_2 = 0.787\,\text{mm}$ with the same parameters as mentioned in the earlier section. To make sensor contact less with LUT, fluidic channels made of transparent polypropylene (PP) material with $(\epsilon_r) = 2.2$ [7] and diameter 4 mm are used. The foam of 0.5 mm height is used between EBG and $50\,\Omega$ microstrip line as shown in Figs. 7 and 8. The LUT, butan-1-ol, methanol, and water are injected by using syringe from one side of the PP tube and collected from the another side to avoid the LUT wastage [7]. The testing of each LUT done with separate PP tube to maintain the purity [7]. The measured S_{12} for no sample, butan-1-ol, methonal, and water are shown in Fig. 8. The resonance frequencies of f_{01}, f_{02}, for no sample, and each LUT are summarised in Table 1. The discrepancies between simulated and measured results are due to humidity effect, fab-
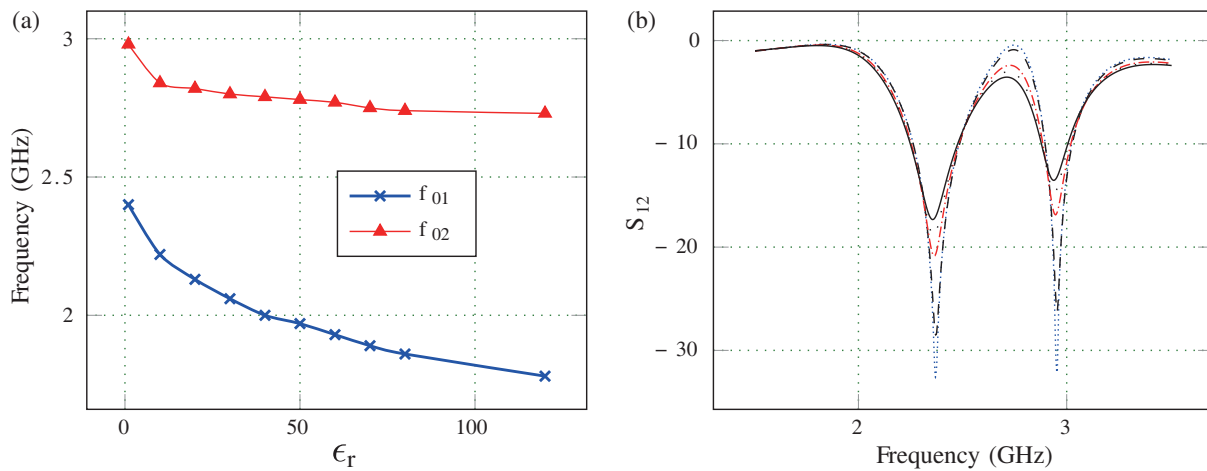
FIGURE 6. (a) Effect of dielectric constant (ϵ_r) on first and second resonance of proposed sensor with $\tan \delta = 0$, (b) Simulated dependence of S_{12} of proposed sensor with loss tangent with $\epsilon_r = 2$. ($\cdots\cdots$ $\tan \delta = 0$, $---$ $\tan \delta = 0.1$, $-\cdot-\cdot-$ $\tan \delta = 0.5$, $\cdots\cdots$ $\tan \delta = 0.7$, ——— $\tan \delta = 0.9$).
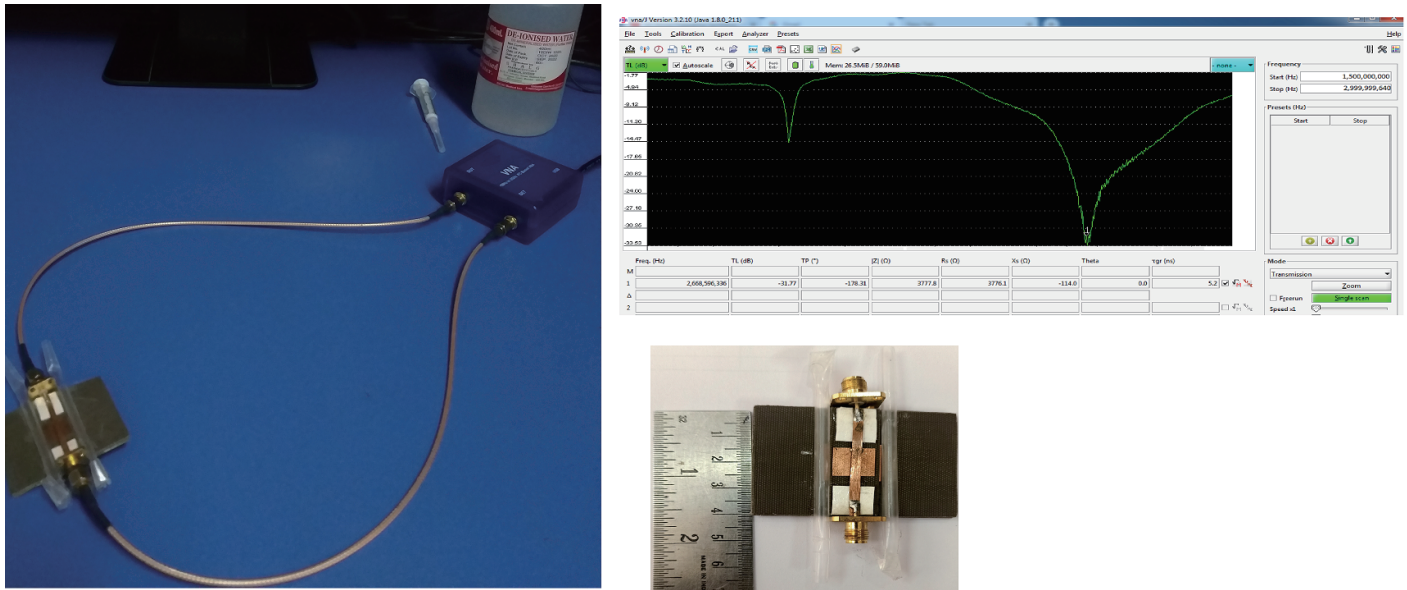

FIGURE 7. Experimental setup, fabricated prototype with empty fluidic channels of proposed SD-EBG based microwave sensor for dielectric characterization of LUT.

rication error, soldering, and results of the possible variation in the measurements [7].

4. PERFORMANCE EVALUATION OF PROPOSED EBG BASED SENSOR

In this section, the performance evaluation of the proposed microwave EBG based sensor in terms of sensitivity (S), Frequency detection Resolution (FDR), and Q-factor with dielectric characterization of different LUT is given.

4.1. Sensitivity, FDR and Q-Factor

Numerical performance evaluation of the proposed EBG based sensor in terms of sensitivity, FDR, and Q-factor for different LUT is summarised in Table 1. A microwave sensor sensitivity

(%) is given as [16, 17]

$$S = \frac{(f_0 - f_s)}{f_0} \frac{1}{\Delta \epsilon_r} (\%) \qquad (5)$$

where f_0 and f_s are the resonating frequency when channels are empty and filled with LUT, respectively. $\Delta \epsilon_r = \epsilon_s - \epsilon_0$, ϵ_0 = dielectric constant of air, and ϵ_s = dielectric constant of LUT. From (5), the considered EBG based sensor demonstrates sensitivities of 1.14%, 0.565%, and 0.278% for butanol-1, Methanol, water for the first resonance, respectively. For the second resonance, it demonstrates sensitivities of 0.921%, 0.298%, and 0.134% for said samples, respectively. It is observed that compared to the first resonance, the second resonance gives less sensitivity. Furthermore, FDR of the proposed sensor for rela-

TABLE 1. Summary of performance analysis of the proposed SD-EBG based sensor for chosen LUT.

LUT name	Resonance Freq. (GHz)		Freq. shift (GHz)		Sensitivity (%)		Q-Factor		FDR (MHz)		Calculated (ϵ_r)		Calculated ($\tan\delta$)	
	f_{01}	f_{02}	1st	2nd	1st	2nd	1st	2nd	1st	2nd	1st	2nd	1st	2nd
No sample (air, $\epsilon_r = 1$)	2.40	2.98	-	-	-	-	-	-	-	-	-	-	-	-
Butan-1-ol, ($\epsilon_r = 3.55$)	2.33	2.91	0.07	0.07	1.14	0.921	29	41	27.4	27.4	3.57	3.58	0.47	0.470003
Methonal, ($\epsilon_r = 22.38$)	2.11	2.79	0.29	0.19	0.565	0.298	8.7	39.42	13.56	8.8	21.3	21.31	0.65	0.650026
Water, ($\epsilon_r = 78.8$)	1.88	2.67	0.52	0.31	0.278	0.134	31.8	137.5	6.68	3.98	78	78.077	0.123	0.123002

1st = First Resonance, 2nd = Second Resonance
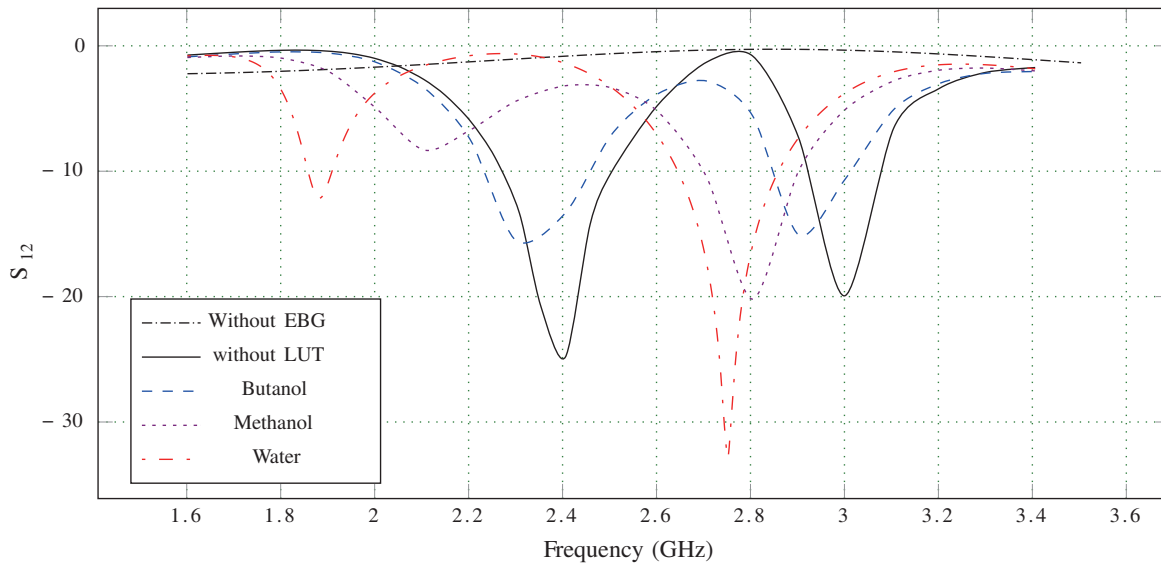

FIGURE 8. Measured S_{12} of proposed SD-EBG based sensor with different LUT.

tives dielectric variation is given as [21]

$$\text{FDR} = \frac{(f_0 - fs)}{\Delta\epsilon_r} \, (\text{GHz}) \qquad (6)$$

for the proposed sensor from experimental results, maximum FDR for the first and second resonances is 0.0274 GHz. Mathematically, Q factor is given as [7]

$$Q = \frac{f_0}{\Delta f} \qquad (7)$$

where $\Delta f = 3\,\text{dB}$ bandwidth and f_0 = resonating frequency. From the numerical analysis for the proposed sensor, maximum Q-factors for the first resonance and second resonance are 31.8 and 137.5, respectively. Compared to reported EBG based sensors, the proposed sensor gives higher Q factor, %S and FDR. From perturbation theory [7, 35], the resonance frequency shift for different LUT and sensitivity depends on the intensity of electromagnetic fields. The Q factor of the sensor depends on the average stored electric and magnetic energies. From simulated results, compared to reported EBG based sensors the average electric field increases, and therefore sensors give higher intensity of electric fields. Thus, sensitivity, FDR, and Q factor of the proposed sensor are improved.

4.2. Dielectric Characterization of Different LUT

Curve fitting technique is an appropriate mathematical model for dielectric characterization of LUT [19]. As discussed in earlier section, the proposed EBG based sensor gives variation in f_0 and $-3\,\text{dB}$ bandwidth Δf for both the bands with respect to the change in ϵ_r and $\tan\delta$ of LUT, respectively. The relation between the variation in the (f_0) and the change in the ϵ_r of LUT for both the bands is expressed using third order polynomial expression.

$$\epsilon_r = 5868.944 - 7263.869 f_{01} + 3011.425 f_{01}^2 - 418.1471 f_{01}^3 \quad (8)$$
$$\epsilon_r = 65174.38 - 65733.02 f_{02} + 22108.74 f_{02}^2 - 2479.763 f_{02}^3 \quad (9)$$

where f_{01} and f_{02} are resonating frequency of LUT for the first and second bands, respectively. The relation between the variation in the $\tan\delta$ and the change in $-3\,\text{dB}$ bandwidth Δf of LUT for both the bands is expressed using third order polynomial expression.

$$\tan\delta = 1.101311 - 0.07647948\Delta f_1 + 0.001141812\Delta f_1^2 \\ - 0.0000003555754\Delta f_1^3 \qquad (10)$$
$$\tan\delta = 3.967879 - 0.3880556\Delta f_2 + 0.009842929\Delta f_2^2 \\ - 0.00007161616\Delta f_2^3 \qquad (11)$$
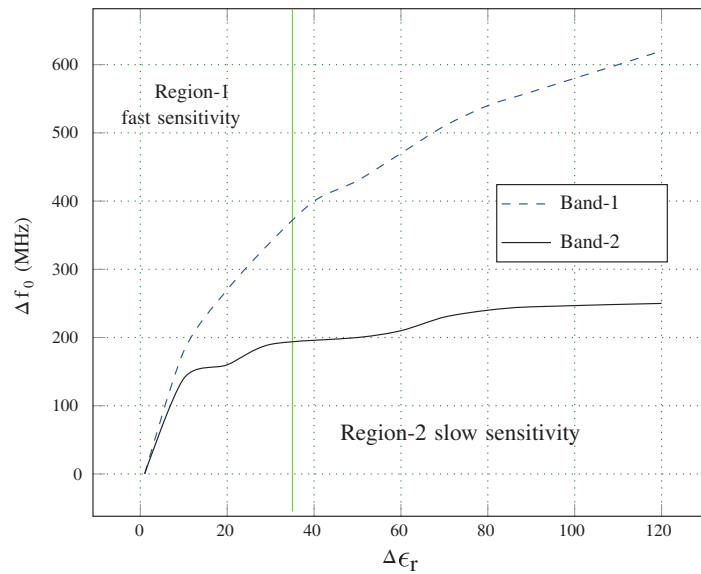
FIGURE 9. Sensitivity of the proposed sensor at both bands.

TABLE 2. Comparison of proposed method with dielectric probe method [32, 33] for dielectric characterization of Liquids.

Dielectric	Methods	LUT		
Properties		Butanol-1	Methonal	Water
Dielectric	DPM	3.55	22.38	78.8
Constant (ϵ_r)	PM	3.57	21.3	78.0
Loss	DPM	0.481	0.62	0.134
Tangent (tan δ)	PM	0.47	0.65	0.123

DPM = Dielectric probe method, PM = Proposed method

TABLE 3. Comparison of proposed work with reported EBG based microwave sensors.

Parameter	[25]	[26]	[7]	**P.W.**
Type of EBG	CLV	square	Cesaro	**Stack**
No. of EBG	2×7	3×3	3×3	**1×1**
Size ($L \times W$), mm^2	140×70	111×111	82×82	**50×40**
ϵ_r	2.2	2.33	2.2	**2.2**
Sensing range of ϵ_r	2–4.4	1–21.3	1–78	**1–78.8**
				1–120*
No. of Resonance	01	01	01	**02**
Max. Q-factor	NM	22.7	90.05	**31.8@**
				137.5#
Max.% S	NM	0.858	0.875	**1.14@**
				0.921#
FDR (MHz)	NM	24.5	21.0	**27.40**

P. W. = Propose work, NM = not mentioned, * from simulation 120, @ for first resonance, # for second resonance.

where Δf_1 and Δf_2 are 3 dB bandwidth for different LUT for the first and second bands, respectively. Table 1 summarizes the sensing performance of the proposed SD-EBG based sensor experimentally in terms of frequency shift, percentage sensitivity, Q factor, and calculated values of ϵ_r and tan δ from (8)–(11). From the experimental results, the proposed sensor has a wide detection range for liquids with $\epsilon_r = 1$ to 78.8 with a maximum Q factor = 31.8 and 137.5 with water as LUT for the first band and second band, respectively. As shown in Fig. 9, the first band gives more sensitivity than the second band. In fast sensitivity region, the percentage sensitivity 1.14 and 0.921 for butan-1-ol is observed for the first band and second band,

respectively, while in slow sensitivity region, percentage sensitivity 0.278 and 0.134 for water as LUT is observed for the first band and second band, respectively. To validate the EBG based sensors fitting function and its calculated results comparison with standards methods like dielectric probe method [32, 33] are provided in Table 2, which shows that proposed sensor to characterize the liquids is in good agreement with the state of the art measurement techniques. The comparison between reported EBG based microwave sensors and proposed dual band, compact SD-EBG based sensor is demonstrated in Table 3.

5. CONCLUSION

In this paper, a dual band and compact SD-EBG based microwave sensor for dielectric characterization has been proposed and experimentally validated. The proposed sensor is composed of suspended microstrip line and unit cell of dual band stack type EBG with operating frequency at 2.40 GHz and 2.98 GHz. To achieve the compact and dual band gap EBG, stack type two EBG patches with different sizes are used. A unit cell of SD-EBG as a resonator with dual band capability is used in design of the sensor, which gives a compact microwave senor. To validate its sensing performance, the absolute solutions of butan-1-ol, methonal, and water are considered as LUT, loaded in cost effective PP pipe and maximum measured sensitivity of 1.14%, maximum measured Q factor 137.5 with frequency detection resolution 27.4 MHz obtained. The size of proposed SD-EBG based sensor is 54.95% and 39.02% of that of planar EBG based sensor and cesaro fractals EBG based sensor.

REFERENCES

[1] Rodríguez-Moré, Z. O., H. Lobato-Morales, R. A. Chávez-Pérez, and J. L. Medina-Monroy, "Complex dielectric permittivity of rum and its mixtures with methanol, ethanol, and water at frequencies up to 15 GHz," *Journal of Microwave Power and Electromagnetic Energy*, Vol. 52, No. 1, 16–30, Jan. 2018.

[2] Torrealba-Meléndez, R., M. E. Sosa-Morales, J. L. Olvera-Cervantes, and A. Corona-Chávez, "Dielectric properties of beans at ultra-wide band frequencies," *Journal of Microwave Power and Electromagnetic Energy*, Vol. 48, No. 2, 104–112, 2014.

[3] Née Haase, N. M., G. Fuge, H. K. Trieu, A.-P. Zeng, and A. F. Jacob, "Miniaturized transmission-line sensor for broadband dielectric characterization of biological liquids and cell suspensions," *IEEE Transactions on Microwave Theory and Techniques*, Vol. 63, No. 10, 3026–3033, Oct. 2015.

[4] Costanzo, S., "Non-invasive microwave sensors for biomedical applications: New design perspectives," *Radioengineering*, Vol. 26, No. 2, 406–410, 2017.

[5] Samant, H., A. K. Jha, and M. J. Akhtar, "Design of coplanar dual band resonator sensor for microwave characterization of dispersive liquids," in *2015 IEEE MTT-S International Microwave and RF Conference (IMaRC)*, 249–252, Hyderabad, India, Dec. 2015.

[6] Su, L., J. Mata-Contreras, P. Vélez, A. Fernández-Prieto, and F. Martín, "Analytical method to estimate the complex permittivity of oil samples," *Sensors*, Vol. 18, No. 4, 984, Mar. 2018.

[7] Arif, A., A. Zubair, K. Riaz, M. Q. Mehmood, and M. Zubair, "A novel Cesaro fractal EBG-based sensing platform for dielectric characterization of liquids," *IEEE Transactions on Antennas and Propagation*, Vol. 69, No. 5, 2887–2895, 2021.

[8] Narayanan, P. M., "Microstrip transmission line method for broadband permittivity measurement of dielectric substrates," *IEEE Transactions on Microwave Theory and Techniques*, Vol. 62, No. 11, 2784–2790, Nov. 2014.

[9] Akhter, Z. and M. J. Akhtar, "Free-space time domain position insensitive technique for simultaneous measurement of complex permittivity and thickness of lossy dielectric samples," *IEEE Transactions on Instrumentation and Measurement*, Vol. 65, No. 10, 2394–2405, Oct. 2016.

[10] Subbaraj, S., V. S. Ramalingam, M. Kanagasabai, E. F. Sundarsingh, Y. P. Selvam, and S. Kingsley, "Electromagnetic non-destructive material characterization of dielectrics using EBG based planar transmission line sensor," *IEEE Sensors Journal*, Vol. 16, No. 19, 7081–7087, Oct. 2016.

[11] Jankovic, N. and V. Radonic, "A microwave microfluidic sensor based on a dual-mode resonator for dual-sensing applications," *Sensors*, Vol. 17, No. 12, 2713, Nov. 2017.

[12] Ansari, M. A. H., A. K. Jha, Z. Akhter, and M. J. Akhtar, "Multi-band RF planar sensor using complementary split ring resonator for testing of dielectric materials," *IEEE Sensors Journal*, Vol. 18, No. 16, 6596–6606, Aug. 2018.

[13] Ebrahimi, A., J. Scott, and K. Ghorbani, "Differential sensors using microstrip lines loaded with two split-ring resonators," *IEEE Sensors Journal*, Vol. 18, No. 14, 5786–5793, Jul. 2018.

[14] Vélez, P., K. Grenier, J. Mata-Contreras, D. Dubuc, and F. Martín, "Highly-sensitive microwave sensors based on open complementary split ring resonators (OCSRRs) for dielectric characterization and solute concentration measurement in liquids," *IEEE Access*, Vol. 6, 48 324–48 338, 2018.

[15] Chuma, E. L., Y. Iano, G. Fontgalland, and L. L. B. Roger, "Microwave sensor for liquid dielectric characterization based on metamaterial complementary split ring resonator," *IEEE Sensors Journal*, Vol. 18, No. 24, 9978–9983, Dec. 2018.

[16] Javed, A., A. Arif, M. Zubair, M. Q. Mehmood, and K. Riaz, "A low-cost multiple complementary split-ring resonator-based microwave sensor for contactless dielectric characterization of liquids," *IEEE Sensors Journal*, Vol. 20, No. 19, 11 326–11 334, Oct. 2020.

[17] Ebrahimi, A., J. Scott, and K. Ghorbani, "Ultrahigh-sensitivity microwave sensor for microfluidic complex permittivity measurement," *IEEE Transactions on Microwave Theory and Techniques*, Vol. 67, No. 10, 4269–4277, Oct. 2019.

[18] Haq, T., C. Ruan, S. Ullah, and A. K. Fahad, "Dual notch microwave sensors based on complementary metamaterial resonators," *IEEE Access*, Vol. 7, 153 489–153 498, 2019.

[19] Acevedo-Osorio, G., E. Reyes-Vera, and H. Lobato-Morales, "Dual-band microstrip resonant sensor for dielectric measurement of liquid materials," *IEEE Sensors Journal*, Vol. 20, No. 22, 13 371–13 378, Nov. 2020.

[20] Fan, L.-C., W.-S. Zhao, D.-W. Wang, Q. Liu, S. Chen, and G. Wang, "An ultrahigh sensitivity microwave sensor for microfluidic applications," *IEEE Microwave and Wireless Components Letters*, Vol. 30, No. 12, 1201–1204, Dec. 2020.

[21] Kiani, S., P. Rezaei, and M. Navaei, "Dual-sensing and dual-frequency microwave SRR sensor for liquid samples permittivity detection," *Measurement*, Vol. 160, 107805, Aug. 2020.

[22] Omer, A. E., G. Shaker, S. Safavi-Naeini, K. Ngo, R. M. Shubair, G. Alquié, F. Deshours, and H. Kokabi, "Multiple-cell microfluidic dielectric resonator for liquid sensing applications," *IEEE*

Sensors Journal, Vol. 21, No. 5, 6094–6104, 2021.

[23] Garcia-Banos, B., F. Cuesta-Soto, A. Griol, J. M. Catala-Civera, and J. Pitarch, "Enhancement of sensitivity of microwave planar sensors with EBG structures," *IEEE Sensors Journal*, Vol. 6, No. 6, 1518–1522, Dec. 2006.

[24] Yadav, R. and P. N. Patel, "Experimental study of adulteration detection in fish oil using novel PDMS cavity bonded EBG inspired patch sensor," *IEEE Sensors Journal*, Vol. 16, No. 11, 4354–4361, Jun. 2016.

[25] Jafari, F. S. and J. Ahmadi-Shokouh, "Industrial liquid characterization enhancement using microwave sensor equipped with electronic band gap structure," *AEU — International Journal of Electronics and Communications*, Vol. 82, 152–159, 2017.

[26] Jun, S. Y., B. S. Izquierdo, and E. A. Parker, "Liquid sensor/detector using an EBG structure," *IEEE Transactions on Antennas and Propagation*, Vol. 67, No. 5, 3366–3373, May 2019.

[27] Peng, L. and C.-L. Ruan, "UWB band-notched monopole antenna design using electromagnetic-bandgap structures," *IEEE Transactions on Microwave Theory and Techniques*, Vol. 59, No. 4, 1074–1081, Apr. 2011.

[28] Zhang, S., "Novel dual-band compact his and its application of reducing array in-band RCS," *Microwave and Optical Technology Letters*, Vol. 58, No. 3, 700–704, 2016.

[29] Sievenpiper, D., L. Zhang, R. F. J. Broas, N. G. Alexopolous, and E. Yablonovitch, "High-impedance electromagnetic surfaces with a forbidden frequency band," *IEEE Transactions on Microwave Theory and Techniques*, Vol. 47, No. 11, 2059–2074, Nov. 1999.

[30] Yang, F. and Y. Rahmat-Samii, "Microstrip antennas integrated with electromagnetic band-gap (EBG) structures: A low mutual coupling design for array applications," *IEEE Transactions on Antennas and Propagation*, Vol. 51, No. 10, 2936–2946, Oct. 2003.

[31] Remski, R., "Analysis of photonic bandgap surfaces using Ansoft HFSS," *Microwave Journal*, Vol. 43, No. 9, 190–199, 2000.

[32] Gregory, A. P. and R. N. Clarke, "Tables of the complex permittivity of dielectric reference liquids at frequencies up to 5 GHz," *CETM, Teddington, U. K., Nature Phys. Rep.*, Jan. 2012.

[33] Abdolrazzaghi, M., M. Daneshmand, and A. K. Iyer, "Strongly enhanced sensitivity in planar microwave sensors based on metamaterial coupling," *IEEE Transactions on Microwave Theory and Techniques*, Vol. 66, No. 4, 1843–1855, Apr. 2018.

[34] Yang, L., M. Fan, F. Chen, J. She, and Z. Feng, "A novel compact electromagnetic-bandgap (EBG) structure and its applications for microwave circuits," *IEEE Transactions on Microwave Theory and Techniques*, Vol. 53, No. 1, 183–190, Jan. 2005.

[35] Meng, B., J. Booske, and R. Cooper, "Extended cavity perturbation technique to determine the complex permittivity of dielectric materials," *IEEE Transactions on Microwave Theory and Techniques*, Vol. 43, No. 11, 2633–2636, Nov. 1995.